

Simple and approximate expressions of demagnetizing factors of uniformly magnetized rectangular rod and cylinder

Cite as: Journal of Applied Physics **66**, 983 (1989); <https://doi.org/10.1063/1.343481>

Submitted: 19 August 1988 . Accepted: 31 March 1989 . Published Online: 17 August 1998

M. Sato, and Y. Ishii



View Online



Export Citation

ARTICLES YOU MAY BE INTERESTED IN

Demagnetizing factors for rectangular ferromagnetic prisms

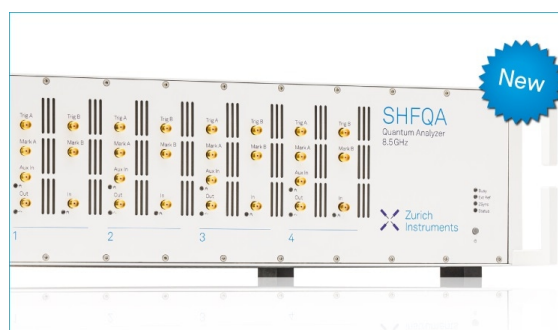
Journal of Applied Physics **83**, 3432 (1998); <https://doi.org/10.1063/1.367113>

Ballistic Demagnetizing Factor in Uniformly Magnetized Cylinders

Journal of Applied Physics **37**, 4639 (1966); <https://doi.org/10.1063/1.1708110>

Demagnetizing Field in Nonellipsoidal Bodies

Journal of Applied Physics **36**, 1579 (1965); <https://doi.org/10.1063/1.1703091>



Your Qubits. Measured.

Meet the next generation of quantum analyzers

- Readout for up to 64 qubits
- Operation at up to 8.5 GHz, mixer-calibration-free
- Signal optimization with minimal latency

Find out more



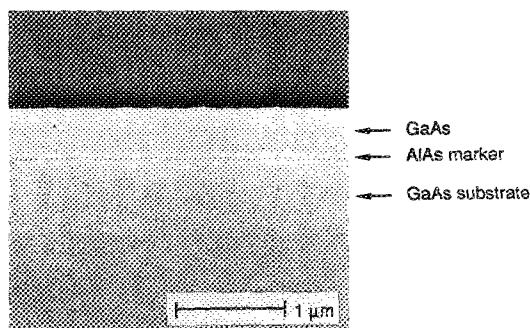


FIG. 2. Scanning electron micrograph cross-section image of the sample of Fig. 1 after the AlGaAs metal liftoff layer has been selectively removed. In the process, the metal mask is also completely removed without disturbing the underlying GaAs layer.

pie after deposition of the Pb/Cr/Au (12000 Å/300 Å/1000 Å) mask by conventional thermal evaporation and photoresist liftoff. Following the implantation, the removal of the metal mask and the AlGaAs cap layer is accomplished simply by etching the sample in hydrochloric acid for 5 min. As shown in Fig. 2, both the metal mask and the AlGaAs cap layer are completely removed. The HCl completely etches the AlGaAs metal liftoff layer, undercutting the metal mask, and causing the metal mask to lift off. The removal of the implantation mask takes place without damage to the surface of the underlying structure, since HCl selectively etches AlGaAs. Examination of the surfaces under lower-power

optical microscopy shows clear featureless surfaces after etching.

In summary, we have described a novel process to fabricate a reliable, easily removed mask for high-energy and high-dose ion implantation. The sample to be implanted is grown with an additional AlGaAs metal liftoff layer as the surface layer, upon which a metal mask is patterned by conventional photoresist liftoff techniques. Following implantation, the AlGaAs metal liftoff layer and the metal mask are removed by selectively etching the AlGaAs with HCl. Due to the selective nature of HCl the underlying epitaxial structure is left undamaged during the removal of the metal mask.

This work was supported by the National Science Foundation Engineering Research Center for Compound Semiconductor Microelectronics (CDR-85-22666), Material Research Laboratory (DMR-86-12860), and the Naval Research Laboratory (N00014-88-K-2005).

¹J. J. Coleman, P. D. Dapkus, C. G. Kirkpatrick, M. D. Camras, and N. Holonyak, Jr., *Appl. Phys. Lett.* **40**, 904 (1982).

²B. Monemar and J. M. Blum, *J. Appl. Phys.* **48**, 1529 (1972).

³P. D. Townsend, *Proc. SPIE* **401**, 295 (1983).

⁴K. V. Vaidyanathan, R. A. Jullens, C. L. Anderson, and H. L. Dunlap, *Solid-State Electron.* **26**, 717 (1983).

⁵D. J. Elliott, *Proc. SPIE* **174**, 153 (1979).

⁶G. Costrini and J. J. Coleman, *J. Appl. Phys.* **57**, 2249 (1985).

⁷L. M. Miller and J. J. Coleman, *CRC Crit. Rev. Solid State Mater. Sci.* **15**, 1 (1988).

Simple and approximate expressions of demagnetizing factors of uniformly magnetized rectangular rod and cylinder

M. Sato

Department of Electronics and Information Engineering, Hokkai-Gakuen University, W-11, S-26, Chuo-ku, Sapporo 064, Japan

Y. Ishii

Department of Electrical Engineering, Hakodate Technical College, Hakodate 042, Japan

(Received 19 August 1988; accepted for publication 31 March 1989)

Demagnetizing factors of the rectangular rod and cylinder magnetized uniformly along the long axis are found to be expressed by the simple and approximate expressions $1/(2n+1)$ and $1/[2(2n/\sqrt{\pi})+1]$, respectively, where n is the dimensional ratio. The error which is the difference of the value evaluated by $1/(2n+1)$ from the value evaluated by the exact expression of the demagnetizing factor is less than 5.48% for the rectangular rod with $n < 70$. The error of the value evaluated by the expression $1/[2(2n/\sqrt{\pi})+1]$ for the cylinder is also found to be less than 4.25% for $n < 100$.

On the studies of magnetization configuration and magnetization reversal process of an elongated ferromagnetic fine particle, it is known that the magnetostatic self-energy plays an important part in the magnetic energy of the particle. The magnetostatic self-energy of an elongated single-domain particle which is magnetized uniformly to saturation is given simply by the expression $N I^2 / 2 \mu_0$, using a

demagnetizing factor N for the direction parallel to the direction of the saturation magnetization I ,¹ where μ_0 is the permeability of the vacuum.

An exact expression of the demagnetizing factor of the uniformly magnetized rectangular rod can be obtained from Eqs. (2.18) to (3.1) in Ref. 2. An exact expression of the demagnetizing factor of the uniformly magnetized cylinder

is given by Brown,³ Eq. (10) in Ref. 4, and Eq. (55) in Ref. 5. Joseph⁶ rederived Brown's result, which is given by Eq. (11) in Ref. 6. These exact expressions of the demagnetizing factors, however, are very complicated to use in the term of the magnetostatic self-energy of the particle. In this work, we obtain simple and approximate expressions of the demagnetizing factors of the uniformly magnetized rectangular rod and cylinder.

We consider a rectangular rod shown in Fig. 1(a). In Fig. 1(a), l and nl are the lengths of the sides of the rectangular rod, and n is the dimensional ratio. When this rectangular rod is magnetized uniformly in the direction of the z axis, we assume the demagnetizing factor N_z of this rod in the direction of the z axis to be proportional to $1/nl$, as in the case of thin films.⁷ Then, $N_z = c/nl$, where c is a proportional constant. When the rectangular rod shown in Fig. 1(a) is magnetized uniformly in the direction of the x or y axes, we obtain $N_x = c/l$ or $N_y = c/l$, where N_x and N_y are the demagnetizing factors of the rod in the direction of the x and y axes, respectively. The proportional constant c is determined by the relation of the demagnetizing factors, $N_x + N_y + N_z = 1$, and we obtain $c = nl/(2n + 1)$. Using $c = nl/(2n + 1)$, we obtain N_x , N_y , and N_z as

$$N_x = N_y = n/(2n + 1) \quad (1a)$$

and

$$N_z = 1/(2n + 1), \quad (1b)$$

which are the simple and approximate demagnetizing factors of the rectangular rod shown in Fig. 1(a).

The values of N_z evaluated from Eq. (1b), which are denoted by a in Table I, and the values of N_z evaluated from the exact expression given by Rhodes and Rawlands,² which are denoted by b in Table I, are given in Table I. The percentage difference between a and b relative to b , $[(a - b)/b] \times 100$, are also given in Table I.

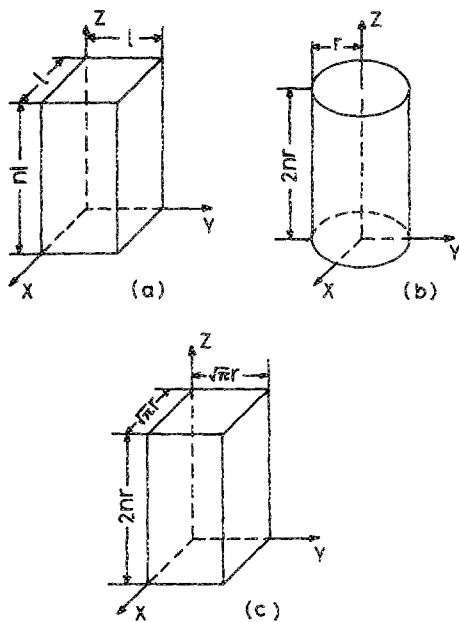


FIG. 1. Rectangular rod and right-circular cylinder.

TABLE I. Demagnetizing factor in a uniformly magnetized rectangular rod N_z . a is evaluated from Eq. (1b) and b is evaluated from the exact expression given by Rhodes and Rowlands (Ref. 2). The percentage difference is $[(a - b)/b] \times 100$.

Dimensional ratio n	N_z		Percentage difference
	a	b	
0.1	0.833333	0.805078	3.51
0.2	0.714286	0.694194	2.89
0.3	0.625000	0.612439	2.05
0.5	0.500000	0.495922	0.82
0.7	0.416667	0.415742	0.22
1	0.333333	0.333333	0.00
2	0.200000	0.198316	0.85
3	0.142857	0.140363	1.78
5	0.090909	0.088316	2.94
7	0.066667	0.064363	3.58
10	0.047619	0.045731	4.13
12	0.040000	0.038330	4.36
15	0.032258	0.030839	4.60
20	0.024390	0.023262	4.85
30	0.016393	0.015595	5.12
50	0.009901	0.009398	5.35
70	0.007092	0.006724	5.48
100	0.004975	0.004684	6.21

Next, we consider a right-circular cylinder with the radius r and length $2nr$, which is shown in Fig. 1(b). To obtain the demagnetizing factor of this cylinder, we replace the cylinder by a rectangular rod with the area of the cross section equal to that of the cylinder, and the replaced rod is shown in Fig. 1(c). The lengths l_x , l_y , and l_z of the sides of the replaced rectangular rod become $\sqrt{\pi}r$, $\sqrt{\pi}r$, and $2nr$, respectively, as seen in Fig. 1(c). According to the same procedure as that to obtain N_x , N_y , and N_z of the rectangular rod shown in Fig. 1(a), we obtain the simple and approximate demagnetizing factor N_x , N_y , and N_z of the rectangular rod shown in Fig. 1(c) as

$$N_x = N_y = (2n/\sqrt{\pi})/[2(2n/\sqrt{\pi}) + 1] \quad (2a)$$

and

$$N_z = 1/[2(2n/\sqrt{\pi}) + 1]. \quad (2b)$$

These demagnetizing factors N_x , N_y , and N_z given by Eqs. (2a) and (2b) are also the simple and approximate demagnetizing factors of the right-circular cylinder shown in Fig. 1(b).

The values of N_z evaluated from Eq. (2b), which are denoted by a' in Table II, and the values of N_z evaluated from the exact expression, Eq. (10) in Ref. 4, are denoted by b' in Table II, are given in Table II. The percentage difference between a' and b' relative to b' , $[(a' - b')/b'] \times 100$, are also given in Table II.

It is found in Tables I and II that the results obtained by the simple and approximate expressions given by Eqs. (1b) and (2b) well agree with the results obtained by the exact expressions^{2,4,6} of the demagnetizing factors. The percentage difference of N_z given by Eq. (2b) is less than 4.25% as seen in Table II. Therefore, the expression given by Eq. (2b) can be used as a simple expression of the demagnetizing factor of the cylinder instead of the complicated expression given by

TABLE II. Demagnetizing factor in a uniformly magnetized cylinder N_z . a' is evaluated from Eq. (2b) and b' is evaluated from the exact expression given by Arrott *et al.* (Ref. 4). The percentage difference is $[(a' - b')/b'] \times 100$.

Dimensional ratio n	N_z		Percentage difference
	a'	b'	
0.1	0.815876	0.796677	2.41
0.2	0.689013	0.680175	1.30
0.3	0.596293	0.594731	0.26
0.5	0.469841	0.474490	-0.98
0.7	0.387637	0.393310	-1.44
1	0.307054	0.311577	-1.45
2	0.181372	0.181864	-0.27
3	0.128696	0.127769	0.73
5	0.081408	0.079907	1.88
7	0.059533	0.058086	2.49
10	0.042431	0.041193	3.01
12	0.035611	0.034501	3.22
15	0.028693	0.027739	3.44
20	0.021675	0.020908	3.67
30	0.014555	0.014008	3.91
50	0.008784	0.008438	4.10
70	0.006290	0.006038	4.19
100	0.004412	0.004232	4.25

Arrott *et al.*^{4,5} and Joseph.⁶ It is also found that the values of the demagnetizing factor of the cylinder, which are given in the text of Bozorth⁸ and are cited in many texts^{9,10} are different from those estimated from the exact expression^{4,5,6} of the demagnetizing factor of the cylinder.

¹C. Kittel and J. Galt, in *Solid State Physics*, edited by F. Seitz and D. Turnbull (Academic, New York, 1956), Vol. 3, p. 502.

²P. Rhodes and G. Rawlands, *Proc. Leeds Philos. Lit. Soc. Sci. Sect. 6*, 191 (1954).

³W. F. Brown, Jr., *Magnetostatic Principles in Ferromagnetism* (North-Holland, Amsterdam, 1962). See the Appendix and Tables A1, A2, and A3.

⁴A. S. Arrott, B. Heinrich, T. L. Templeton, and A. Aharoni, *J. Appl. Phys.* **50**, 2387 (1979).

⁵A. S. Arrott, B. Heinrich, and A. Aharoni, *IEEE Trans. Magn.* **MAG-15**, 1228 (1979).

⁶R. I. Joseph, *J. Appl. Phys.* **37**, 4639 (1966).

⁷S. Middelhoek, *J. Appl. Phys.* **34**, 1054 (1963).

⁸R. M. Bozorth, *Ferromagnetism* (Van Nostrand, Reinhold, New York, 1951), p. 845.

⁹S. Chikazumi, *Physics of Magnetism* (Wiley, New York, 1964), p. 19.

¹⁰K. Ohta, *Zikikohgaku no Kiso I* (Kyohritsu Shuppan, Tokyo, 1973), p. 38 (in Japanese).

Rocking curve peak shift in thin semiconductor layers

C. R. Wie

State University of New York at Buffalo, Department of Electrical and Computer Engineering, Bonner Hall, Amherst, New York 14260

(Received 20 February 1989; accepted for publication 5 April 1989)

A simple x-ray diffraction method for determining layer composition and mismatch is by measurement of the separation of peaks in a rocking curve. This method can only be used for layers with a thickness above a certain value. This minimum thickness can be significantly large for layers with a small lattice mismatch as in AlGaAs/GaAs or isoelectronic-doped III-V semiconductor layers. We give such an example and show that the interference between the diffraction amplitudes of the thin layer and that of the substrate is responsible for the peak shifting of the layer Bragg peak. When this peak shifting is significant, the kinematical diffraction theory and the peak separation method should not be used for the mismatch measurement, and only the dynamical diffraction theory simulation should be used. We present a criterion on the layer thickness, below which the dynamical theory simulation must be used. This thickness is inversely proportional to the lattice mismatch and does not depend on the diffraction geometry, wavelength, and substrate material.

Lattice mismatch and film composition of semiconductor heterojunction epitaxial layers are commonly measured by x-ray diffraction.¹⁻³ A quick and easy method is by measuring the separation of peaks in the rocking curve, from which the lattice mismatch and composition are calculated by considering the unit cell distortion and Vegard's law.⁴ Fewster and Curling⁵ showed a few examples of rocking curves for which the peak separation method is invalid due to the peak-shifting effect caused by the substrate or by other thicker layers. They did not, however, explain the exact cause of such peak shifting nor gave any criterion for what samples the peak separation method should not be used. Un-

derstanding the exact cause of the peak shifting is important for determining whether any approximation made in a diffraction model is valid or not.

Figure 1(a) shows the 004 $\text{CuK}\alpha_1$ rocking curves of a GaAs epitaxial layer doped with an isoelectronic dopant (In), grown on a GaAs(001) substrate by liquid phase epitaxy (LPE). The isoelectronic doping technique is used to improve III-V epitaxial layer quality by reducing the background dislocation and electron trap densities.⁶ The rocking curves in Fig. 1(a) are taken from an as-grown sample (curve a) and after successive 2-min chemical etching (curves b, c, and d). These curves have been reported in Ref.